Journal of Knot Theory and Its Ramifications, Vol. 3 No. 3 (Special Issue, 1994) 263–278

KNOTTING OF REGULAR POLYGONS IN 3-SPACE

KENNETH C. MILLETT
Department of Mathematics
University of California
Santa Barbara, CA 93106
millett@math.ucsb.edu

Received 31 January 1994
Revised 1 July 1994

ABSTRACT

The probability that a linear embedding of a regular polygon in $\mathbf{R}^3$ is knotted should increase as a function of the number of sides. This assertion is investigated by means of an exploration of the compact variety of based oriented linear maps of regular polygons into $\mathbf{R}^3$. Asymptotically, an estimation of the probability of knotting is made by means of the HOMFLY polynomial.

Keywords: polygonal knots, random, knot spaces

0. Introduction

Although the concept of an isometric linear embedding of a polygon in $\mathbf{R}^3$, a polygonal knot, has always been a facet of knot theory, recently the subject has taken on new life with stimulus from efforts to study the possible shapes of macromolecules such as DNA. Here the vertices correspond to the atoms or collections of atoms and the edges correspond to the bonding between them. In the case of a relatively homogeneous macromolecule, the model could be based on the regular polygon. This is the principal case considered in this paper.

The central question is the determination of the key properties of the space of various types of polygonal knots. There are many qualities that one might wish to ascribe to such knots, such as allowing differing edge lengths, restrictions on angles between edges, or even restrictions on an "energy" associated to potential configurations. Each knot space consists of the collections of all knots having the specified properties. This space can be represented as a collection of points in an appropriate Euclidean space defined by the family of constraints determining the properties of the knots under consideration.

A principal reference for the basic concepts is Randell, [1 & 2]. Randell, [1], asked "Suppose one takes a random polygonal simple closed curve in three-space so that all n edges have equal length. What is the probability that it will be knotted?" This is the main question investigated in this work.

The underlying mathematical concepts are presented in the first section. The walk algorithm is discussed in the second section and, in the third section, the results of the computer simulation are presented.

1. Geometric and Topological Knotting

Let $\mathcal{M}^n$ denote the space of based oriented maps into $\mathbf{R}^3$ of the regular planar n-gon (whose edges have length one) which are linear and length preserving on the edges and which take the base vertex to (0,0,0) and the next vertex (in the direction determined by the orientation) to (1,0,0). Each point of $\mathcal{M}^n$ is represented by the image of the vertices of the n-gon, $\{(0,0,0),(1,0,0),x_3,\ldots,x_n\}$. $\mathcal{M}^n$ can be represented by the set of points $\{x_3,\ldots,x_n\} \in (\mathbf{R}^3)^{n-2}$ with $\|x_i - x_{i+1}\| = 1$, $1 \leq i \leq n-1$, $\|x_n - x_1\| = 1$. This is a compact $(2n-5)$-dimensional real semialgebraic variety.

Singular maps are those for which the images of two edges meet in an interior point of each or the image of an edge meets the image of a vertex which is not one of its vertices. The set of singular maps in $\mathcal{M}^n$ is a real semialgebraic set, $\mathcal{S}^n$, because it is described by a finite family of polynomial equations and inequalities.

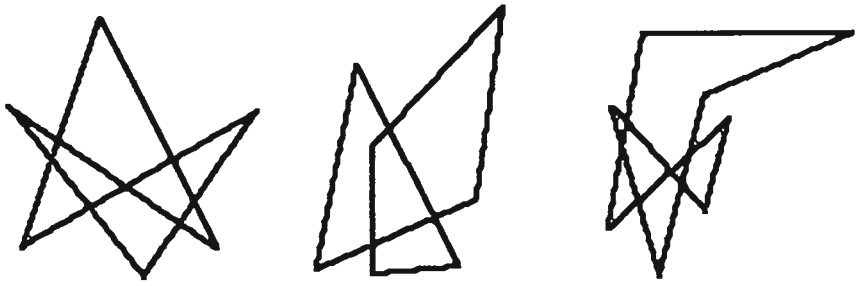

FIG. 1.1

Let $\mathcal{K}^n = \mathcal{M}^n - \mathcal{S}^n$ denote the subspace consisting of those maps which determine embeddings of the regular n-gon. For $n = 6$, 7 and 8, examples of typical trefoil knot projections are shown in Figure 1.1. The components $\mathcal{K}^n$ are $(2n-5)$-dimensional non-compact manifolds whose topology and geometry is determined by their situation in $\mathbf{R}^{3(n-2)}$. The closure of these manifold components contain singular maps. For example, except in the initial case of $n = 4$, the codimension one singularities consists of maps which are immersions with a single double point interior to each of two edges, such as shown in Figure 1.2.

Theorem 1.1 (Randell [2]). *$\mathcal{M}^n$ is a manifold if n is odd. When n is even, $\mathcal{M}^n$ has singular points (not having manifold neighborhoods) occurring when all edges are collinear. $\mathcal{K}^n$ is always a manifold.*

The components of $\mathcal{K}^n$ define the **geometrical knot types** of these regular n-gons. There are finitely many knot types since differences of semialgebraic varieties have finitely many path components, [3]. Because this introduces a nonstandard

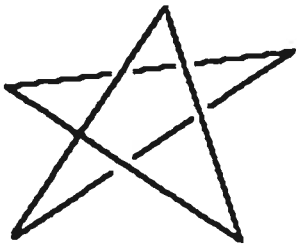

FIG. 1.2

notion of knot equivalence, symbols such as "K" and "L" are used to denote a specific spatial configuration. When the geometrical knot type determined by K is required, this will be made explicit. Similarly, with regard to the topological knot type determined by K, explicit mention of this usage will be made. Let $\mathcal{K}_0^n$ denote the subspace consisting of spatial polygons which are topologically unknotted. In general, if $r.s$ denotes the s^{th} knot with r crossings in a knot table, e.g. Rolfsen [4], the $\mathcal{K}_{r.s}^n$ will denote the union of components of K^n consisting of knotted polygons which are topologically equivalent to $r.s$.

Proposition 1.2.

(1) $\mathcal{M}^3 = \mathcal{K}^3 = \mathbf{S}^1$
(2) $\mathcal{M}^4 \supset \mathcal{K}^4 = \mathcal{K}_0^4 = \mathbf{S}^1 \times (int\ \mathbf{D}^2)$.
(3) $\mathcal{M}^5 \supset \mathcal{K}^5 = \mathcal{K}_0^5$ *is path connected.*[1]
(4) *(i)* $\mathcal{K}^6$ *has at least 3 components and (ii)* $\mathcal{K}_0^6$ *is connected.*[2]

$\mathcal{M}^4$ is a 3-dimensional real algebraic variety whose codimension one skeleton is the wedge of two 2-spheres, $\mathbf{S}^2 \vee \mathbf{S}^2$, at the "south poles" and whose codimension two skeleton consists of the cone point and the two "north poles." A neighborhood of each of the codimenison two points consists of a cone on a torus. $\mathcal{K}^4$ is the product of a circle with an open disk. The "coordinates" are illustrated in Figure 1.3.

If one factors out the effect of the rotation about the x-axis, the quotient of $\mathcal{K}^4$ is an open disk whose closure is the 2-disk shown in Figure 1.4. There is an arc of singular maps connecting the center to the radius along which the ϕ angle is equal to zero. Along the opposite radius this angle is π. The limit of embeddings approaching the boundary of the disk are singular maps with a fixed ϕ angle which varies from 0 to 2π as one moves around the circumference of the boundary circle.

It is not known if $\mathcal{K}_{r.s}^n$ is connected nor is there an explicit example which demonstrates that it is not connnected. In addition, there are no systematic means to determine the minimum number of edges required to realize a given knot type as a linearly embedded regular polygon. Note, however, that if a given knot can be realized then so also is its mirror reflection, by virtue of the involution of the variety taking a map to its mirror reflection through the x-y plane.

[1] Randell [1]
[2] This fact is joint work with Rosa Orellana

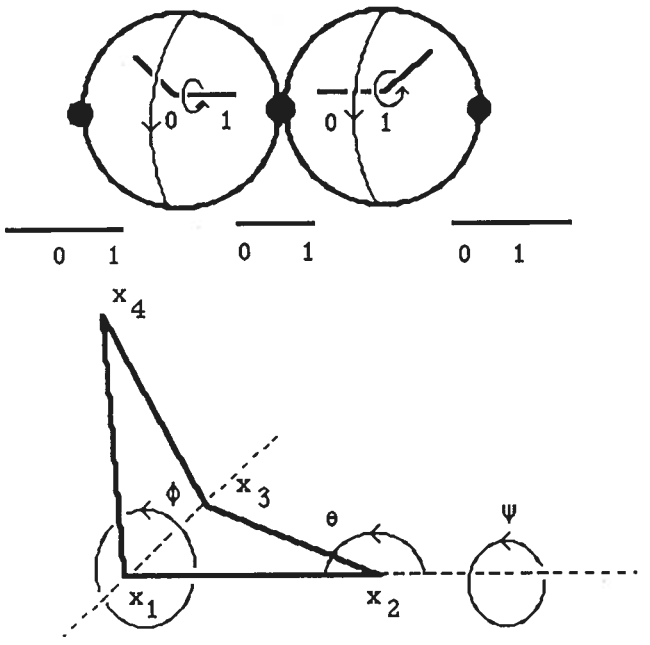

FIG. 1.3

Proposition 1.3. *The trefoil knot can be constructed as a regular hexagon. The figure eight knot can be constructed with seven edges. The knots* 5_2 *and* 6_2 *can be constructed with eight edges.*

Table 1. Coordinates of Some Polygonal Knots

3_1 (Trefoil)

1. {0., 0., 0.}
2. {0.944977, 0.267782, −0.187912}
3. {0.167581, 0.781216, 0.175462}
4. {0.493272, 0.639999, −0.759409}
5. {0.610324, 0., 0.}
6. {0.30516, 0.918868, −0.250113}

4_1 (Figure Eight):

1. {0., 0., 0.}
2. {0.604096, −0.58404, 0.216761}
3. {0.0967492, −0.0853225, −0.280128}
4. {0.913614, 0., 0.}
5. {0.187253, −0.463355, −0.103546}
6. {0.808807, −0.167237, 0.424664}
7. {0.675628, −0.35646, −0.411685}

5_2

1. {0., 0., 0.}
2. {0.403918, 0.57239, −0.713596}
3. {0.807837, 0., 0.}
4. {1.21111, −0.129158, 0.905918}
5. {0.818382, −0.187695, 0.0118714}
6. {0.16972, 0.404907, −0.465685}
7. {0.243271, −0.592336, −0.455838}
8. {0.991404, −0.014265, −0.13006}

6_2

1. {0., 0., 0.}
2. {0.623368, −0.103103, −0.775101}
3. {0.277732, −0.261129, 0.149866}
4. {0.510008, −0.980900, −0.5043345}
5. {0.782871, −0.313936, 0.1889945}
6. {−0.17666, −0.223485, −0.077689}
7. {0.794947, 0., 0.}
8. {0.397473, −0.90626, −0.143905}

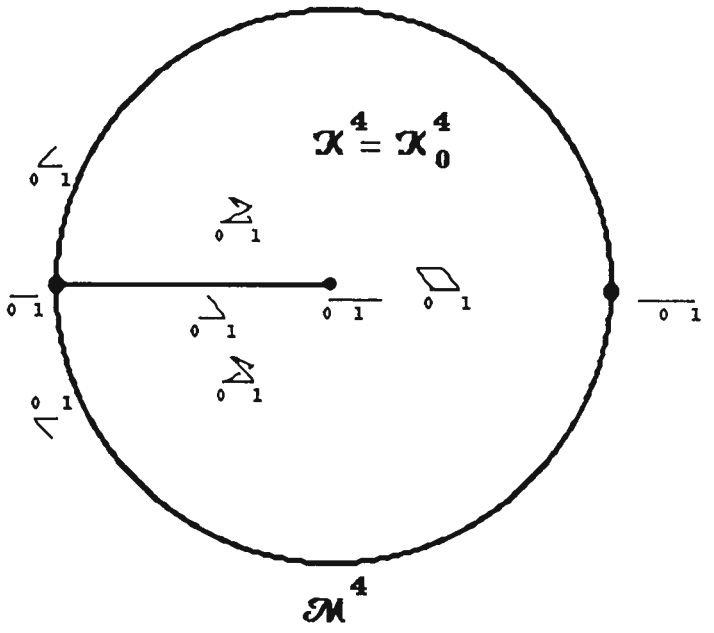

FIG. 1.4

Conjecture 1.4: All of the five and six crossing knots can be constructed as knotted regular octagons.

It is a classical result that the trefoil requires at least six edges. A simple geometric argument shows that the Figure 8 knot requires at least seven edges. The evidence for this conjecture is that physical models of these knots have been constructed which seem to have sufficient 'freedom of motion' that they suggest the "mathematical existence." In the case of the octagons, only one case of the knots 5_2 and 6_2, given above, were encountered in 3,270,987 samples taken as part of the walk simulation reported later in this paper. On the other hand, there were 8,804 trefoil knots and 226 figure knots realized as knotted octagons.

Table 2.

	Models Constructed	Computer Coordinates Determined
3_1	6	6
4_1	7	7
5_1	8	9
5_2	8	8
6_1	8	10
6_2	8	8
6_3	8	11

Coordinates for all examples of 2-fold connected sums of right handed and left handed trefoils have been found with 11 vertices. Geometrical considerations show

that they can be easily constructed with 10 vertices. It seems likely that one would not require even as many as 10 vertices to realize the connected sum of two right trefoils. Note that many of the elementary questions, such as this, of classical knot theory can become challenging problems in this setting. For example, it is unlikely that the connected sum decomposition of a knot is independent of the order or method of its construction. This occurs because the standard method of proof of independence requires the ability to alter the scale of the knot, a process prohibited by the definition of the regular polygonal knot.

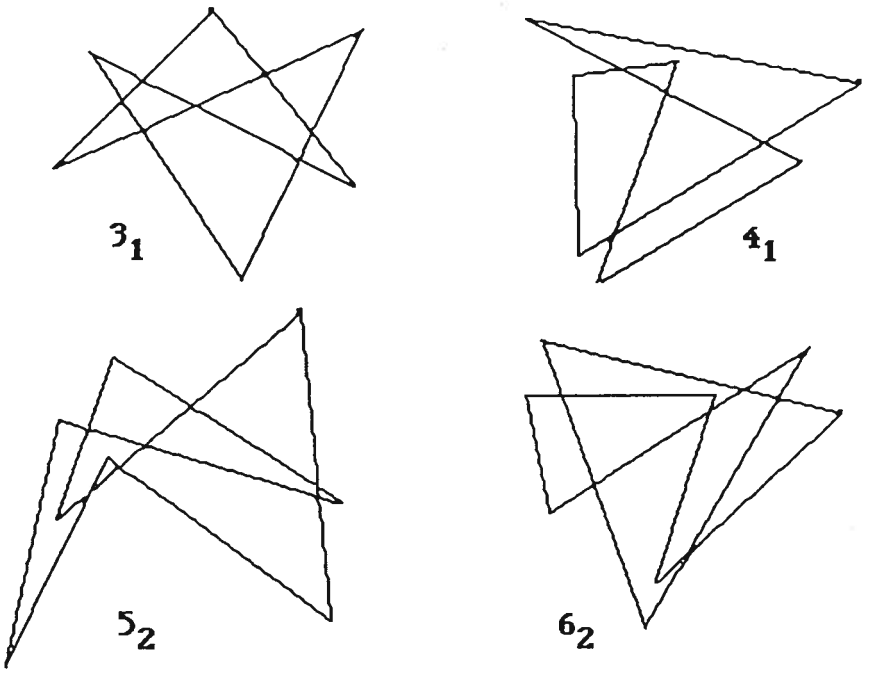

FIG. 1.5

Recall that the bridge number, $\beta(K)$, of a knot is the minimum number of maxima with regard to a height function on K. In the topological setting, this minimum is taken over all smooth realizations of K. In the geometric setting one has the same notion except that one must use geometrically equivalent realizations of K with "n" edges giving a new bridge number, $\beta(K)_n$. $\beta(K)_n \geq \beta(K)$, with equality occurring for sufficiently large n.

If K is a polygonal knot of n edges one can define the total curvature of K as the sum of the exterior angles at the n vertices of K, $\kappa(K)$.

Theorem 1.5 (Milnor [5]). $k(K) \leq 2\pi\beta(K)$.

Corollary 1.6. *If $\kappa(K) < 4\pi$, then K is topologically unknotted.*

Question 1.7: If $\kappa(K) < 4\pi$, then is K geometrically unknotted?

The specification of a fixed number of edges places limitations on the geometric complexity and, therefore, on the range of topological knot types that can be realized. For example, $\kappa(K) \leq n\pi$ and $\beta(K)_n \leq [n/2]$. Thre are only a finite number of configurations possible for a generic projection of an object formed on n segments of fixed lengths. Since each of the crossings is either under or over (and ther are significant geometric limitations here as well), there are only a finite number of geometric knot types that can be constructed with any given number of segments. Current estimates, however, do not provide useful information concerning the actual number of geometric knot types that can be realized with a given number of edges.

The following data refers to the knots shown in Figure 1.5.

Table 3.

Knot	Model n	Curvature	$\beta(K)_n$
3_1	6	14.0230	2
4_1	7	17.1504	2
5_2	8	17.8430	2
6_2	8	18.8542	2

2. Walks and Knotting

A walk in $\mathcal{K}^n$ can be constructed as follows:

- The polygonal knot, K, is determined by the set of vertices $\{(0,0,0),(1,0,0), x_3,\ldots,x_n\}$.
- According to a uniform distribution, select two distinct non-adjacent vertices, x_i and x_j, of the polygonal knot, k. They separate the polygon into two non-trivial components.
- Hold one of these components fixed, rotate the other component about the axis determined by the two vertices through an angle selected according to a uniform distribution.
- If necessary, translate the base vertex to (0,0,0) and then rotate the second vertex to (1,0,0) to determine a point in $\mathcal{M}^n$.
- If the map is an element of $\mathcal{K}^n$, accept the result. If not, repeat the process until an element of $\mathcal{K}^n$ is created.

In order to use this walk as a means of exploring the variety, the following proposition is necessary.

Proposition 2.1. *Given any pair of knots, K and K', there is a walk connecting K to K'.*

Proof. It is sufficient to show that any configuration can be created from the standard one by a sequence of these operations. Suppose that $K = \{(0,0,0),(1,0,0),x_3,..$ $x_n\}$ is the standard regular planar n-gon and $K' = \{x'_1, x'_2, x'_3, \ldots, x'_n\}$ is any element of $\mathcal{K}^n$.

Step 1. Move K' to a planar configuration. First translate the configuration until x'_1 is at (0,0,0) and rotate about the origin so that x'_2 is at (1,0,0). The remaining steps are accomplished by rotations about axes connecting x'_1 to successive vertices beginning at x'_2. Rigidly rotate the portion from x'_2 to x'_n about the

axis determined by x_1' and x_2' until x_3' lies in the first quadrant of the x-y plane. Continuing, rotate the portion from x_3' to x_n' about the axis determined by x_1' and x_3' until x_4' lies in the portion of the x-y plane (determined by the axis) which does not contain x_2'. The exceptional case in which x_4' lies on the axis does not require a rotation to be made. Continue in this fashion to create a planar configuration of the type shown in Figure 2.1. Except in the exceptional cases in which an edge lies on the axis connecting x_i' to x_{i+1}', each edge corresponds to a sector determined by successive axes.

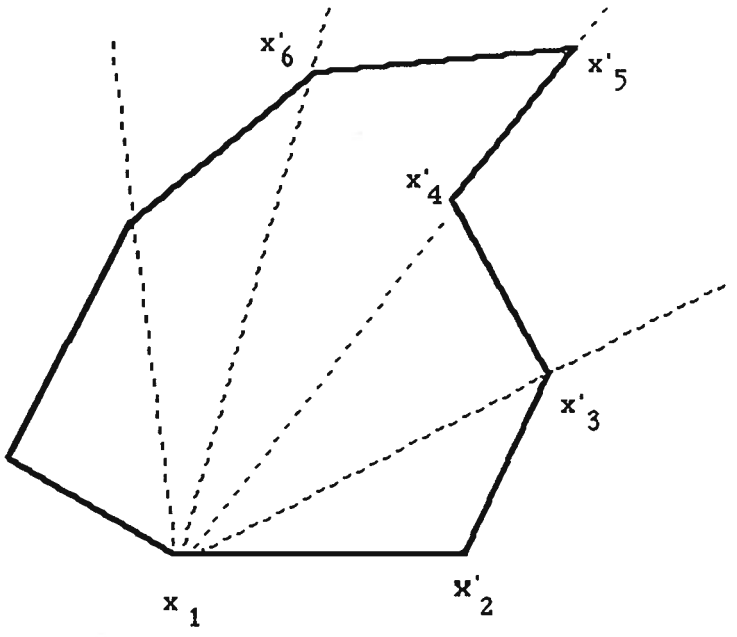

FIG. 2.1

Step 2. Move to a convex planar configuration by rotations along the edges. This can be accomplished by making rotations along the edges such as illustrated in Figure 2.2 because a configuration is convex if and only if all the segments connecting the vertices lie within the figure. Equivalently, each of the exterior angles must be positive, i.e. counter clockwise. The previous construction ensured that this was the case for the first three vertices. Suppose, by induction, that this is case for the first i vertices and not the $i+1^{\text{st}}$. This means that the exterior angle determined by the edge connecting the $i-1^{\text{st}}$ to the i^{th} and the edge connecting the i^{th} to the $i+1^{\text{st}}$ is negative. Rotating about the axis defined by the $i-1^{\text{st}}$ and the $i+1^{\text{st}}$ vertices changes the sense of the exterior angle so that it is now positive. Unfortunately, however, this may have changed the sense of the angle at the $i-1^{\text{st}}$ vertex. If this is the case one rotates about the axis defined by the $i-2^{\text{nd}}$ and the i^{th} vertices. The effect of these rotations is to produce an edge connecting the edge i^{th} to the $i+1^{\text{st}}$ vertex which is parallel to the original edge connecting the edge $i-1^{\text{st}}$ to the i^{th} vertex. The ultimate effect is the creation

of a configuration in which all exterior angles are positive for vertices 1 through $i+1$. An exceptional case arises when the vertex in question is the first vertex. The rotation has as its axis the first vertex and the $n-1^{st}$ vertex. Proceed as above until all angles are positive or the edge in question has become the first edge. This, however, is impossible as this creates a polygon congruent to the original polygon but with strictly more area because each of the rotations adds area to the polygon. Thus a convex polygon must have been created earlier.

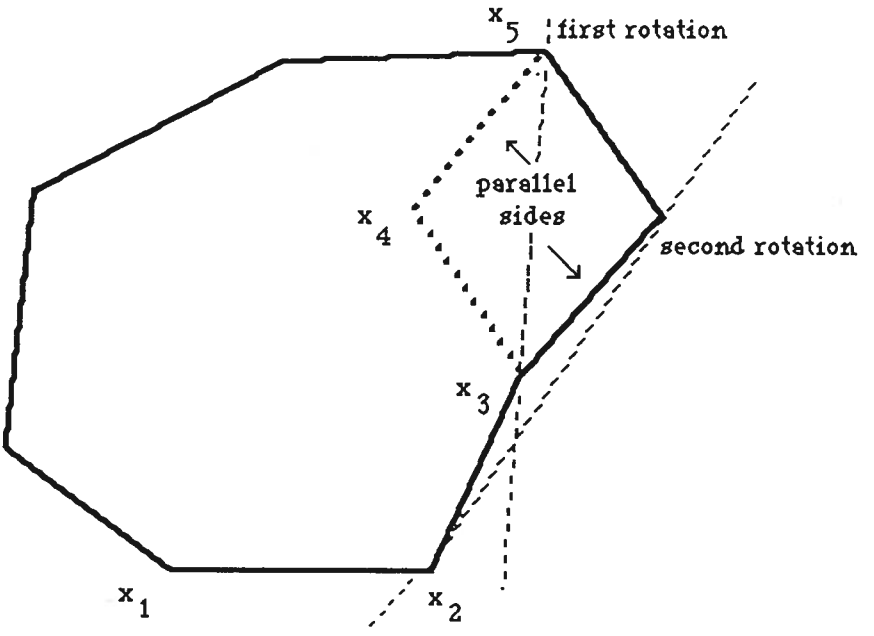

FIG. 2.2

Step 3. Move to the standard position. The goal is to now fix the angles or, equivalently, to fix the distances between the successive edges so that the result is the standard polygon. The sum of the interior angles is constant, equalling $(n-2)\pi$, with the regular polygon having angles equalling the target value of $(n-2)\pi/n$. The proof is accomplished by increasing the number of vertices in a sequence at which the angles equal the target value. The first step is show that, if there is not already such a vertex, one may be constructed. There must be some angles larger and some angles smaller than the target value. Select an adjacent pair consisting of one of each. The typical case is shown in Figure 2.3. Suppose that the angle at C is too small and the angle at B is too large.

By rotating about axis BD the distance AC can be made to equal the distance which determines the target angle. The angle at B is now equal to the target value. This places C at C'. By rotating about the axis AC' the vertex B can be moved to B' which is co-planar with A, C' and, D. This does not change the size of the angle. By rotating about the axis AD, the vertices B' and C' can be moved to B'' and C'' lying in the plane of the original figure. The angle at B'' equals the target

value.

The number of vertices not contained in the sequence having standard angles must be four or more. Suppose the minimal case is shown in Figure 2.3. The distance AD must equal the corresponding distance in the standard polygon. One of the angles among B and C must be smaller than the target value, the other larger. The previous argument makes both equal to the target value and completes the proof in this special case.

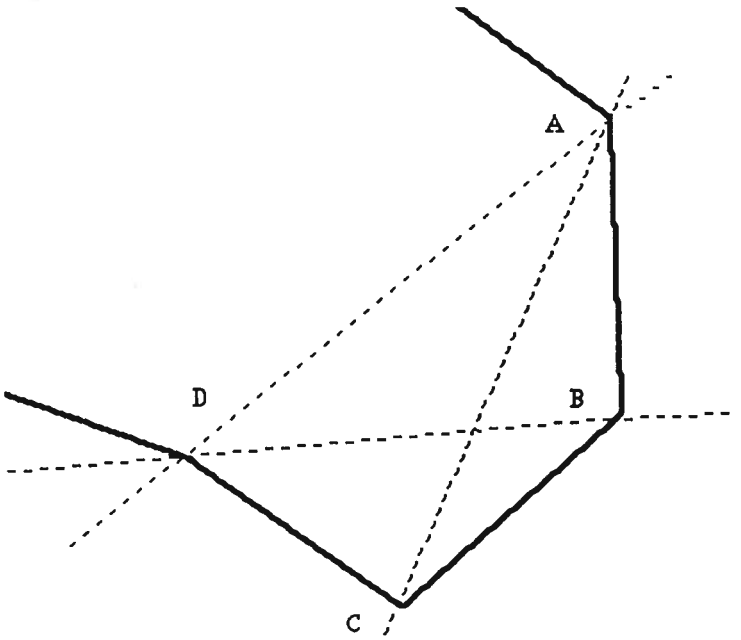

FIG. 2.3

Suppose that there is a sequence of five or more vertices not contained in the target sequence. The vertices with standard angles are numbered 1 through i. The goal is to make the angle at the $i+1^{st}$ vertex standard. The portion of the angle determined by i, $i+1$ and n is standard as that portion of the polygon is congruent with a standard polygon. The goal, then, is to move the angle determined by $i+2$, $i+1$ and n to the complementary angle necessary to make the angle at i standard. This is accomplished by a series of rigid rotations about various axes. By rotating about axes $i+1 : i+2$, $i+1 : i+3$, etc. the angle $n : i+1 : i+2$ can be modified. The extent of this modification is controlled by the angle between $i+1 : i+2$ and the axis. This angle can be modified by rigid rotations about $n : i+3$, $n : i+4$, etc. followed by a rotation about $i+1 : i+3$, $i+1 : i+4$, respectively. As a consequence, the angle $n : i+1 : i+2$ can be made equal to the correct complementary angle. However, the positions of $i+2$, $i+3$, etc. may no longer be in the initial plane. This is accomplished by first using rotations about $n : i+2$, $n : i+3$, etc. to move the vertices into the plane determined by $i+1$, $i+2$, and n. Rotation about the

$n : i+1$ axis returns the vertices to the initial plane without changing the angle $i+2 : i+1 : n$. As a result, the angle at $i+1$ is now standard. □

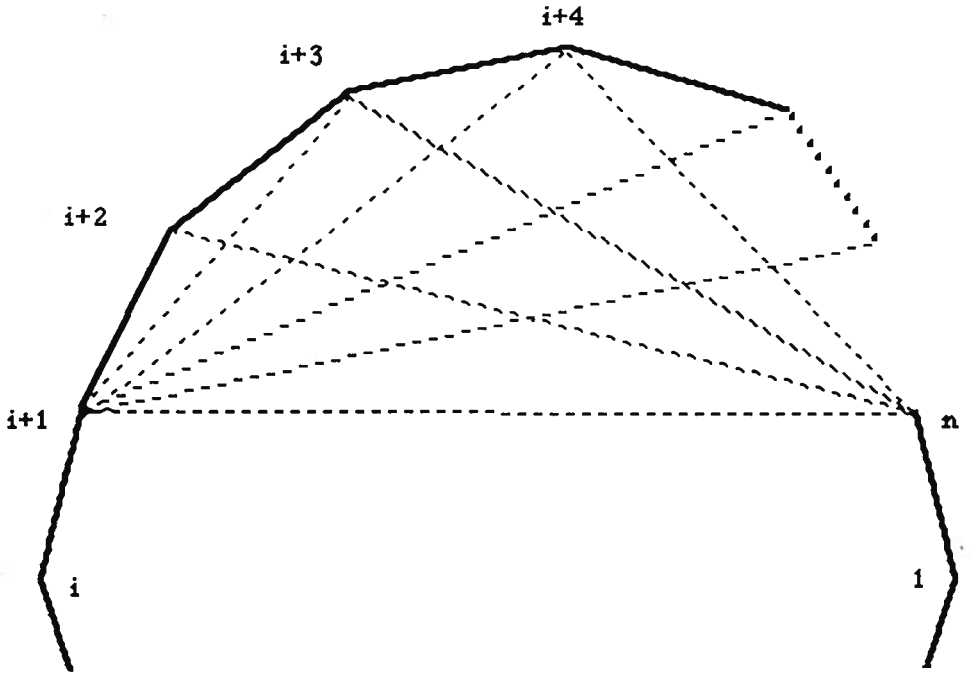

FIG. 2.4

3. Computer Simulations

The first implementation of the walk algorithm was accomplished by Theresa Hughes, as part of her UCSB masters' degree thesis research. It was translated into "C" and optimized by Stefan Boeriu for pilot implementation on various computers. The data reported in this paper came from the pilot investigations of the walk.

The walk algorithm consists of randomly selecting a pair of vertices in the knot, fixing one of the segments they determine, and rotating the other segment about the axis determined by the pair of vertices through a randomly selected angle. The resulting configuration is coded for analysis and the next step is taken. Because of cpu time limitations that walk was broken up into sequences of 100,000 step segments (or, if necessary, smaller), each segment beginning where the previous one ended. The entire walk began at the standard planar configuration. Thus the entire walk began at this base point and was reported in segments, the final position being recorded in the event the walk is to be continued at a later time.

The principal focus of the exploration was to determine the occurrence of knotting as a function of the number of edges. The walk algorithm was run on Sun SPARCstations, on an IBM RISC System/6000 and, on both a Cray YMP and a Cray C90. The code is fully optimized: of a total of 67 inner loops, 60 are vectorized. The unvectorized loops are mainly character operations and their weight

in the CPU usage is low. The CRAY code uses exclusively the CRAY Math and Scientific Library Routines. Using the HPM utility, a speed of 125.64 MIPS has been obtained for a typical case. The ration (speed on a CRAY 90)/(speed on SUN SPARC) is 20 for 25 edges and increases to 100 for a 400 edge case, reflecting the vectorization of the code.

Because of concern with the random number generators, data from these various sources was compared in order to insure that there was no detectable bias within the range of the data collected. Each configuration of points in 3-space was checked to insure that they determined an embedded curve in 3-space and that the projection to the x-y plane was generic and provided a legitimate coding of a knot. Never, in any of the many millions of cases that were generated, was a singular curve or non-generic projection detected. Currently, the computational complexity of the knot generation process is the limiting factor in the simulation.

The sequence of knots, 50,000 to 100,000 per collection, is analyzed by means of the HOMFLY, [6 & 7], polynomial. In the current implementation of the algorithm used to calculate the HOMFLY polynomials there is a constraint to knots or links having presentations with no more than 126 crossings. Cases of this began to appear only in the study of the knots created in 45 edges. There we encountered one every several hundred thousand steps. This was not sufficiently significant to alter the estimation of the prevalence of knotting. For knots arising from 15 edges and 45 edges, the average cpu time for HOMFLY polynomial calculation was about 0.022579 and 0.026833 seconds, respectively, so that their calculation required only about 35 to 45 minutes on a Sun SPARCstation. For small numbers of sides, 6 through 8, the polynomials were found by means of a table accounting for the significant increase in time between 8 and 9 sides. The generation of the examples required approximately 30 minutes on the Cray YMP. The graph in Figure 3.1 shows the average amount of time required to calculate the HOMFLY polynomial of an n edge configuration as a function of n. Although it is known that the calculation HOMFLY polynomial is NP-hard [8], the present simulation seems to indicate that its calculation, contrary to popular belief [9], is nevertheless a powerful tool to apply in the study of knot populations.

The HOMFLY polynomial is a finite Laurent polynomial in two variables, ℓ and m, with integer coefficients associated to each topological knot type. Although not a complete invariant of the knot type, these polynomials are very strong filters of the knot types. Within the range of observed knots, it is a faithful detector of knotting. For example, the polynomial associated to the left-handed trefoil knot is $-2\ell^2 - \ell^4 + \ell^2 m^2$. In many cases, but not all, it detects chirality by means of a lack of invariance under the involution taking ℓ to ℓ^{-1}. In this study we have used the collection of terms involving only ℓ. Among the 2977 knots representable with fewer than 13 crossings, there are 76 cases which might be confused with the trivial knot using this criteria. These are identified separately by looking at the higher order terms in their polynomials.

3.1 Probability of Knotting

Let $\mathbf{p}(n)$ denote the probability that a regular polygon with n edges is knotted. The results of the analysis of each of the sequences of knots generated in the walk is used to estimate $\mathbf{p}(n)$ by computing the frequency or observed probability of

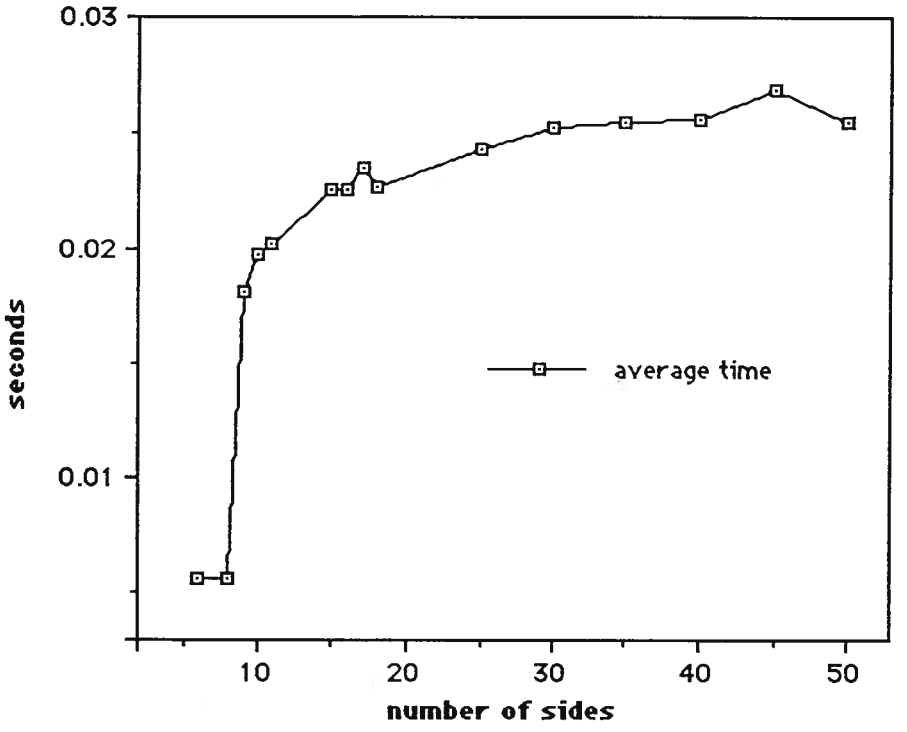

FIG. 3.1

knotting as determined by the initial segment of the walk to that point. One expects these values to converge to $\mathbf{p}(n)$ but, in examples, the rate of convergence appears to be rather slow. As a consequence, some of the reported values have may be only accurate to one or two significant figures. The data for the case of the octagon is shown in Figure 3.2.

The estimation of the probability of knotting calculated in this study provides some information on the qualitative behavior of the polygons with small numbers of edges. The following graph, which shows the results of the pilot calculations, includes data from 6 edges through 20 edges and 25, 30, 35, 40 and 45 edges. A key fact to note from this graph is that the probability function is concave upward in this region. The asymptotic behavior is initiated at an inflection point following which the graph is concave downward. The numerical determination of this transition point is one of the computational goals of this research.

Sumners and Whittington [10] and Pippenger [11] proved independently that the probability that an n edge polygon in $\mathbf{Z}^3$ is knotted goes to 1 exponentially quickly, i.e. $\limsup(1 - \mathbf{p}(n))^{1/n} = e^{-a_0} < 1$. van Rensburg and Whittington, [12], have estimated that $a_0 = (7.6 \pm 0.9) - 10^{-6}$. Although this type of behavior may occur for regular polygons with many edges, calculations show that this is clearly not the case for smaller values of n. Another possibility is a logistic model

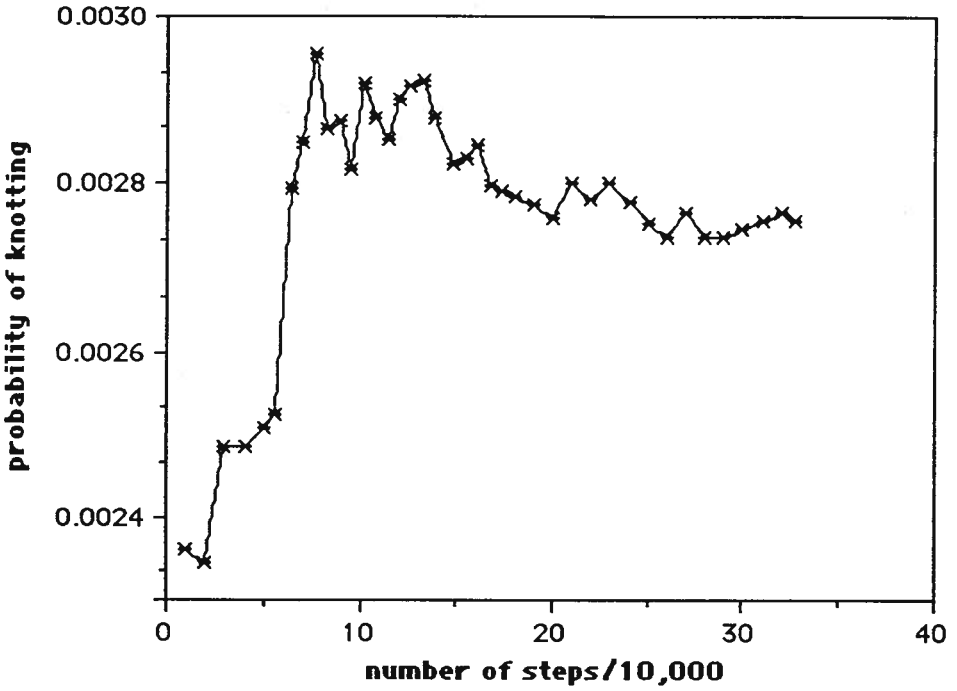

FIG. 3.2

of the form $\mathbf{p}(n) = 1/(1 + Ae^{-kn})$. It has asymptotic growth consistent with the theoretical result for large values of n and has the potential of characterizing the growth of knotting for small values of n. The graph of such a logistic function and the experimental data, Figure 3.4, gives a qualitative sense of why this does not appear to be the case. Diao, Pippenger and, Sumners have similar results in the case of Gaussian random polygonal knots, [13].

With some experimentation it seems more likely that a quadratic function is the one best adapted to the observed data for smaller values of n. The quadratic function used in the graph, Figure 3.5, is $-0.011359+0.001506x+0.00003x^2$. Of course this function only characterizes the small scale behavior of the growth in the probability of knotting for regular spatial polygons. It does suggest that, in this setting, the knotting probability function may reflect various geometric characteristics not encountered in other settings.

Problem: What is the source of the apparent quadratic growth in the probability of knotting for small regular spatial polygons?

Acknowledgements

The computer simulations were undertaken with the assistance of Stefan Boeriu, who translated the walk algorithm into FORTRAN and implemented it on various computers. During this research many knot figures were developed using the

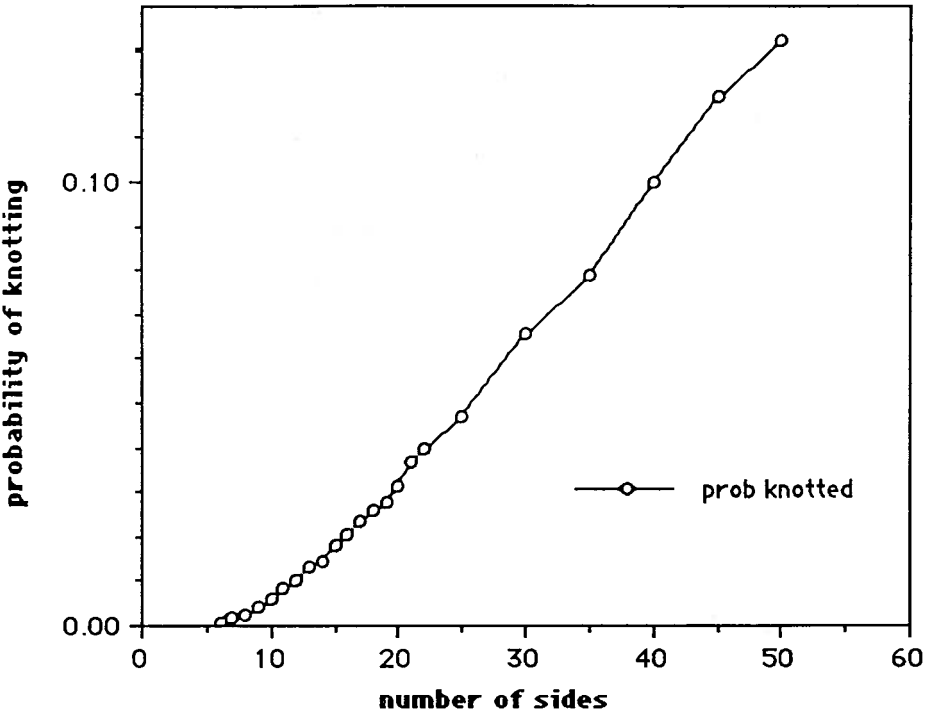
probability of knotting
0.10
0.00
0
10
20
30
40
50
60
number of sides
prob knotted

FIG. 3.3

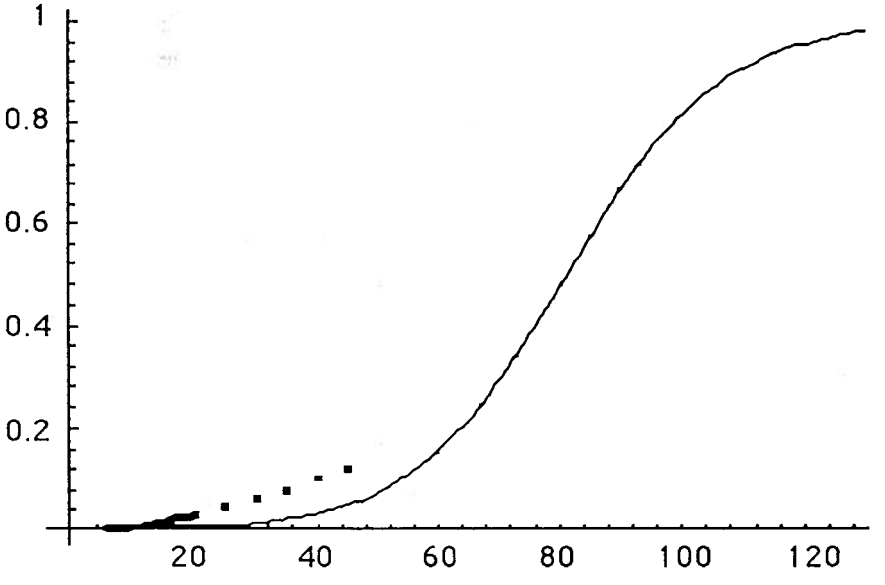
1
0.8
0.6
0.4
0.2
20
40
60
80
100
120

FIG. 3.4

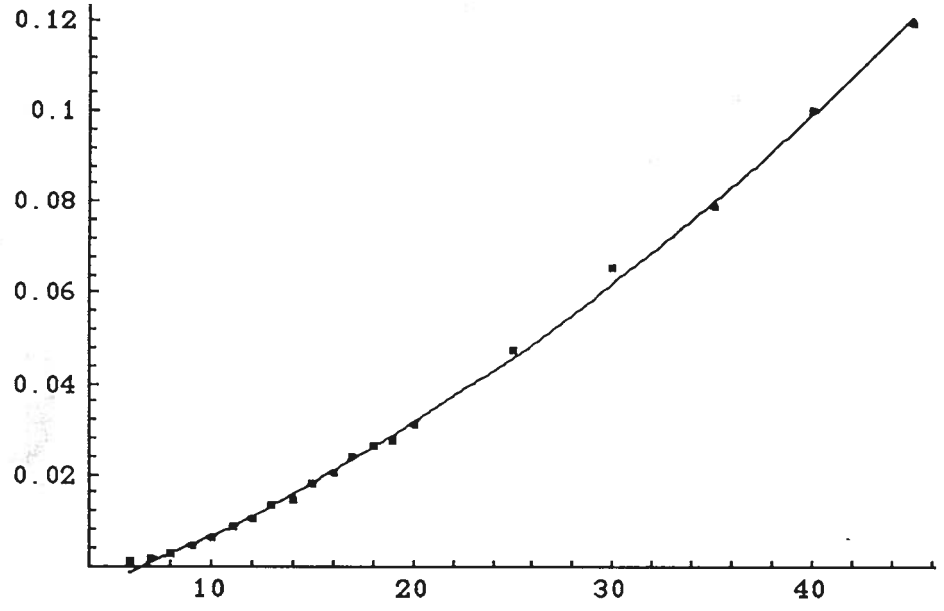

FIG. 3.5

Surface Evolver from the Minnesota Geometry Center, [14]. Assistance of the San Diego Supercomputer Center and the Minnesota Geometry Center is gratefully acknowledged.

REFERENCES

[1] R. Randell, *A molecular conformation space, MATH/CHEM/COMP 1987*, Studies in Physical and Theoretical Chemistry **54** (1988), 125–140.

[2] R. Randell, *Conformation spaces of molecular rings, MATH/CHEM/COMP 1987*, Studies in Physical and Theoretical Chemistry **54** (1988), 125–140.

[3] H. Whitney, *Elementary structure of real algebraic varieties*, Annals of Math **66** (1957), 545–556.

[4] D. Rolfsen, *Knots and Links*, Publish or Perish Press, Berkeley, 1976.

[5] J. Milnor, *On the total curvature of knots*, Ann. Math. **52** (1950), 248–257.

[6] P. Freyd, D. Yetter, J. Hoste, W. B. R. Lickorish, K. C. Millett, and A. Ocneanu, *A new polynomial invariant of knots and links*, Bull. Amer. Math. Soc. **12** (1985), 239–246.

[7] W. B. R. Lickorish and K. C. Millett, *A polynomial invariant of oriented links*, Topology **26** (1987), 107–141.

[8] F. Jaeger, D. L. Vertigan and D. J. A. Welsh, *On the computational complexity of the Jones and Tutte polynomials*, Math. Proc. Camb. Phi. Soc. **108** (1990), 35–53.

[9] T. Deguchi and K. Tsurusaki, *A Statistical Study of Random Knotting Using the Vassiliev Invariants*, talk at the AMS Special Session on Random Knotting and Linking, Vancouver, August 18–19, 1993.

[10] D. W. Sumners and S. G. Whittington, *Knots is self-avoiding walks*, J. Phys. A: Math. Gen. **21** (1988), 1689–1694.

[11] N. Pippenger, *Knots in random walks*, Discrete Appl. Math. **25** (1989), 273–278.

[12] E. J. Janse van Rensburg and S. G. Whittington, *The knot probability in lattice polygons*, J. Phys. A: Math Gen. **23** (1990), 3573–3590.

[13] Y. Diao, N. Pippenger, D. W. Sumners, *On Random Knots*, preprint (1992).

[14] K. Brache, *Surface Evolver Manual*, Research Report GCG55, Minnesota Geometry Center, July 1993.